Semaphorin controls epidermal morphogenesis by stimulating mRNA translation via eIF2α in *Caenorhabditis elegans*

Akira Nukazuka, Hajime Fujisawa, Toshifumi Inada, Yoichi Oda, and Shin Takagi[1]

Division of Biological Science, Nagoya University Graduate School of Science, Chikusa-ku, Nagoya 464-8602, Japan

Conserved semaphorin–plexin signaling systems govern various aspects of animal development, including axonal guidance in vertebrates and epidermal morphogenesis in *Caenorhabditis elegans*. Here we provide in vivo evidence that stimulation of mRNA translation via eukaryotic initiation factor 2α (eIF2α) is an essential downstream event of semaphorin signaling in *C. elegans*. In semaphorin/plexin mutants, a marked elevation in the phosphorylation of eIF2α is observed, which causes translation repression and is causally related to the morphological epidermal phenotype in the mutants. Conversely, removal of constraints on translation by genetically reducing the eIF2α phosphorylation largely bypasses requirement for the semaphorin signal in epidermal morphogenesis. We also identify an actin-depolymerizing factor/cofilin, whose expression in the mutants is predominantly repressed, as a major translational target of semaphorin signaling. Thus, our results reveal a physiological significance for translation of mRNAs for cytoskeletal regulators, linking environmental cues to cytoskeletal rearrangement during cellular morphogenesis in vivo.

[*Keywords*: *C. elegans*; cofilin; eIF2; epidermal morphogenesis; mRNA translation; semaphorin]

Supplemental material is available at http://www.genesdev.org.

Received December 18, 2007; revised version accepted February 27, 2008.

Ligand binding to receptors at the surface of individual cells triggers changes in gene expressions and cytoskeletal organization, which underlies dynamic cellular morphogenesis. The signaling system consisting of semaphorins and their receptor plexins, both in vertebrates and in invertebrates, is involved in the regulation of diverse developmental events including axonal extension and cell migration in the nervous system, growth of endothelial cells, and cardiac development (Kruger et al. 2005).

Elucidation of semaphorin–plexin signaling cascades is paramount for understanding these morphogenetic events. For instance, Sema3A, a secreted semaphorin in vertebrates, triggers collapse or repulsive turning of growth cones as a consequence of asymmetrical alteration in F-actin structure (Fan and Raper 1995). Cytoskeletal regulators, such as Rho family small GTPases (Jin and Strittmatter 1997; Kuhn et al. 1999; Rohm et al. 2000; Zanata et al. 2002; Oinuma et al. 2004; Turner et al. 2004), collapsin response mediator proteins (CRMPs) (Goshima et al. 1995), and an actin-depolymerizing factor (ADF)/cofilin (Aizawa et al. 2001), mediate the growth cone responses by acting as molecular relays to transduce the Sema3A's repulsive signal. In parallel with these demonstrations, great interest has been focused on local mRNA translation occurring in Sema3A-induced axonal events since the discovery by Campbell and Holt (2001).

mRNA translation initiation is the rate-limiting step in the process of protein synthesis, in which eukaryotic initiation factor 2 (eIF2) complex and eIF4F complex formations are the major events. eIF2 forms a ternary complex with GTP and initiator methionyl-tRNA (Met-$tRNA_i^{Met}$) and recruits Met-$tRNA_i^{Met}$ to the ribosome (Hershey and Merrick 2000). Phosphorylation of the α subunit of eIF2 (eIF2α) inhibits global translation, while it also increases translation of a few selected mRNAs (Holcik and Sonenberg 2005). eIF4F complex, composed of eIF4A (RNA helicase), eIF4E (cap-binding protein), and eIF4G (scaffold protein), serves to initiate 5′ cap-dependent translation by recruiting mRNA to the ribosome (Gingras et al. 1999; Hershey and Merrick 2000). Sema3A accelerates protein synthesis locally in growth cones as marked by rapid rises in the phosphorylation of translational regulators eIF4E and 4E-BP1, and pharmacological translation inhibition blocks the Sema3A-induced responses of isolated growth cones (Campbell and Holt 2001), suggesting that Sema3A exerts its navigatory influence through the translational regulation at axonal terminals. Recently, mRNAs for RhoA (Wu et al. 2005), ADF/cofilin (Piper et al. 2006), and β-actin (Leung et al.

[1]**Corresponding author.**
E-MAIL i45116a@nucc.cc.nagoya-u.ac.jp; FAX 81-52-789-2979.
Article is online at http://www.genesdev.org/cgi/doi/10.1101/gad.1644008.

2006) have been identified as targets to be translated in response to Sema3A and other guidance cues such as Slit2 and Netrin-1. Thus, cytoskeletal reorganization mediated by synthesis of cytoskeletal regulators and/or components is suggested to be a fundamental mechanism for cue-induced axonal navigation. In spite of these understandings, however, the functional significance of translational regulation in semaphorin signaling in vivo has not been addressed. In order to gain insight into semaphorin signaling in vivo, we used the genetic analysis in nematode *Caenorhabditis elegans*, where two membrane-bound semaphorins interact with an A-type plexin to regulate morphogenesis of epidermal tissues including the "rays" in the male tail (Fujii et al. 2002; Ginzburg et al. 2002; Dalpe et al. 2004).

In this study, we present several lines of in vivo evidence that the semaphorin–plexin signal regulates the phosphorylation level of eIF2α and stimulates translation. Furthermore, we identify cofilin as a key functional target of translation in response to semaphorin. Our results reveal a physiological significance for regulated translation of mRNA species, especially those relevant to cytoskeletal regulation, which provides some clues to the mechanism that links environmental cues to cytoskeletal reorganization underlying alteration of cell morphology in vivo.

Results

A role for semaphorin–plexin signaling in the epidermal ray morphogenesis

We have shown previously that in *C. elegans* membrane-bound semaphorins (SMP-1 and SMP-2; SMPs) interact with an A-type plexin (PLX-1) to regulate the morphogenesis of epidermal tissues including the rays: nine bilateral pairs of sensilla enveloped in a cuticular fan in the male tail (Fujii et al. 2002; Ginzburg et al. 2002; Dalpe et al. 2004).

In wild-type adults, ray 1, the anterior-most ray, is mostly found juxtaposed to its neighboring ray 2 ("Level 1" phenotype) (Fig. 1A). In contrast, in *plx-1(nc37, ev724)* single and *smp-1(ev715) smp-2(ev709)* double mutant adults, ray 1 is frequently displaced anteriorly (Fig. 1B,C). The displaced ray 1 is often found outside of a fan ("Level 3" phenotype), and in some cases ray 1 is separate from ray 2 within a fan ("Level 2" phenotype) (see Supplemental Fig. S1 for examples of the three levels).

Previous studies showed that the SMPs–PLX-1 system determines the position of ray 1 by regulating the shape and arrangement of epidermal ray precursor cells (Fujii et al. 2002; Ginzburg et al. 2002; Dalpe et al. 2004). On each side of a larval male tail are nine epidermal cell-derived R(n) cells, each of which divides to give rise to Rn.a and Rn.p (n = 1–9). Through successive divisions, each Rn.a becomes a ray precursor cluster comprising three cells that later develops into a mature ray (Sulston et al. 1980; Emmons 2005). Examination of ray precursor cells with the adherens junction marker *ajm-1*::*gfp* (Baird et al. 1991; Mohler et al. 1998) revealed that the ray 1 phenotype in the mutant adults results from the abnormal shaping of R1.p, which consequently affects the arrangement of ray precursor cluster 1 (Fig. 1E–G; Fujii et al. 2002). The ray 1 phenotype in *plx-1* adults is remarkably rescued by driving expression of *plx-1* under the *lin-32* promoter (*lin-32*p) (Fig. 1I; Nakao et al. 2007). Since in larval males the *lin-32*p drives gene expressions pre-

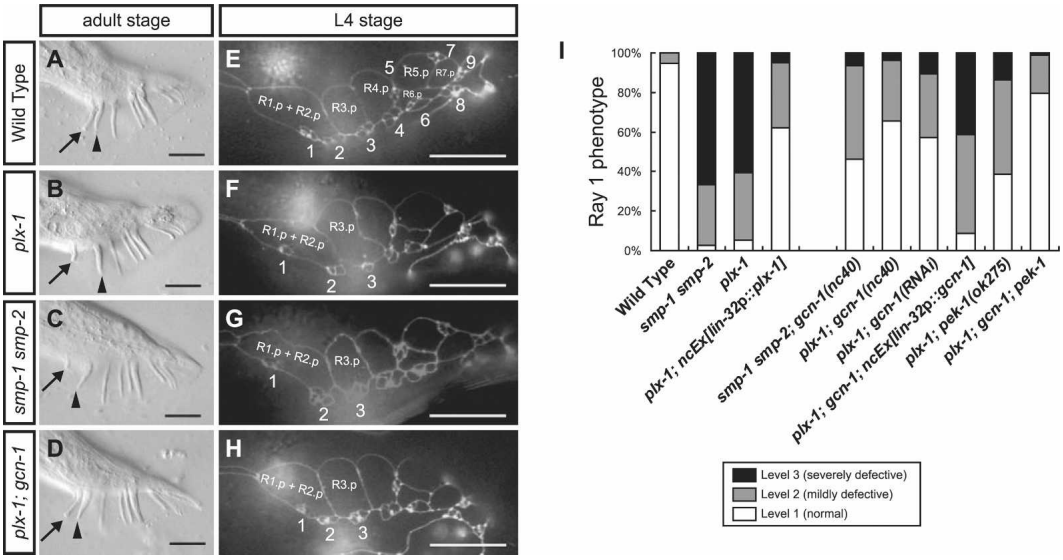

Figure 1. Ray configurations in adults (*A–D*) and in larvae at the L4 stage (*E–H*). Anterior is left, and dorsal is top. Bars, 10 µm. Ray 1 (arrow), which is normally located juxtaposed to its neighboring ray 2 (arrowhead) in wild-type adults (*A*), is found anteriorly in *plx-1* (*B*) and *smp-1 smp-2* (*C*) mutants. (*D*) *gcn-1(nc40)* was isolated as a mutation that suppresses the ray 1 phenotype in *plx-1*. (*E–H*) Configurations of epidermal ray precursor cells visualized with *ajm-1*::*gfp* at the L4 stage, when R1.p and R2.p have already fused. Numbers indicate ray precursor cluster (n), where n = 1–9. (*E*) In wild type, ray precursor cluster 1 is associated with the vicinal cluster 2. In contrast, in *plx-1* (*F*) and *smp-1 smp-2* (*G*), cluster 1 shifts anteriorly. (*H*) In *plx-1; gcn-1*, cluster 1 is located close to cluster 2 as in wild type. (*I*) Quantitative evaluation of the ray 1 phenotype in adult males of the indicated genotypes.

dominantly in nine R(n) cells and their descendants (Supplemental Fig. S2; Portman and Emmons 2000), where expressions of SMPs and PLX-1 overlap (Fujii et al. 2002; Ginzburg et al. 2002), it is likely that the SMPs–PLX-1 signal in epidermal ray precursor cells is responsible for their morphogenesis.

Loss of a GCN1 homolog function suppresses the ray 1 phenotype

To gain insight into SMPs signaling, we conducted a screen for mutations that suppress the ray 1 phenotype in *plx-1* mutants. One isolated mutation, *nc40*, suppressed the ray defect in *plx-1* as well as that in *smp-1 smp-2* mutants (Fig. 1D,H,I). *nc40* single mutants displayed normal ray configuration (Supplemental Tables S1, S2).

nc40 was mapped to the clone Y48G9A on the left arm of linkage group III. Sequencing revealed that *nc40* is a 6880-base-pair (bp) deletion between nucleotides 90,212 and 97,091 on Y48G9A, including four microRNA genes and part of the GCN1 homolog-encoding gene (termed "*gcn-1*") (Supplemental Fig. S3A). We cloned the *gcn-1* cDNA and found the gene to be a composite of *Y48G9A.1*, *Y48G9A.2*, and *Y48G9A.3*, which had been registered as three separate genes in WormBase (http://www.wormbase.org; Supplemental Fig. S3A). RNAi against *gcn-1* in *plx-1* mutants suppressed the ray 1 phenotype, and *lin-32*p-driven *gcn-1* expression markedly reversed the suppression by *nc40* (Fig. 1I), confirming that loss of *gcn-1* function was responsible for suppressing the ray defect in *plx-1*/*smp-1 smp-2* mutants. The sequence corresponding to the 12th and the 13th exons are entirely deleted in the *nc40*-type *gcn-1* transcript, which is presumably translated into a truncated form of GCN-1 protein. The deleted region, between amino acids 895 and 1138, is reportedly necessary for GCN1 function in yeast (Sattlegger and Hinnebusch 2000). In addition, *nc40* in *trans* to a deficiency (*nc40*/*tDf9*) suppressed the ray 1 phenotype in *plx-1* adults equally to the *nc40* homozygotes (Supplemental Table S1), indicating that *nc40* acts genetically as a null allele of *gcn-1*.

GCN1, conserved among eukaryotes (Supplemental Fig. S3B), is known to function as a negative regulator for the translation initiation of global mRNAs (Marton et al. 1993). A trimeric GTPase eIF2, composed of α, β, and γ subunits, forms a ternary complex with GTP and Met-tRNA$_i^{Met}$ and participates in the initiation of translation by recruiting Met-tRNA$_i^{Met}$ to the 40S ribosomal subunit (Hershey and Merrick 2000). In yeast and mammalian cells, GCN1 activates the serine/threonine kinase GCN2 in response to nutrient limitation, which in turn phosphorylates the specific serine residue of eIF2α. On the phosphorylation of eIF2α, eIF2 forms a stable complex with eIF2B, a guanine nucleotide exchange factor, to prevent the recycling between a GDP-bound and a GTP-bound state, and thereby global translation initiation is inhibited (Hinnebusch 2000). Paradoxically, however, the eIF2α phosphorylation also increases the rate of translation of a few selected mRNAs (Holcik and Sonenberg 2005).

The 49th serine residue of a *C. elegans* eIF2α homolog, which is encoded by the *Y37E3.10* gene (Rhoads et al. 2006), is the putative phosphorylation site, as predicted by the complete identity of the surrounding residues among eukaryotes (Supplemental Fig. S4), suggesting the conserved regulatory mechanism of the eIF2α phosphorylation. We carried out Western blot analysis to detect the level of eIF2α phosphorylation (P-eIF2α) in wild-type and *gcn-1* mutant larvae at stage 1 (L1). In *gcn-1* mutants, a reduction in P-eIF2α to 28% of wild type was observed (Fig. 2A), indicating that GCN-1 does participate in the eIF2α phosphorylation.

Loss-of-function mutations in a PERK gene suppress the ray defect

In metazoans, a kinase PERK, which is activated by unfolded protein response, phosphorylates eIF2α at the same residue as GCN1 signaling (Ron and Harding 2000). Although less pronounced than *gcn-1*, loss-of-function mutations in a *C. elegans* PERK homolog, *pek-1* (Shen et al. 2001), also suppressed the ray defect in *plx-1*/*smp-1 smp-2* mutants (Fig. 1I; Supplemental Table S2) and reduced P-eIF2α (Fig. 2A). In addition, the *gcn-1; pek-1* double mutation suppressed the ray 1 phenotype in *plx-1* adults and reduced P-eIF2α more strongly than either single mutation (Figs. 1I, 2A).

The semaphorin signal lowers the eIF2α phosphorylation

The finding that mutations that diminish P-eIF2α suppressed the ray defect in *plx-1*/*smp-1 smp-2* mutants prompted us to examine whether the SMPs signal regulates the ray morphogenesis by controlling P-eIF2α. We first compared P-eIF2α in wild type with that in *plx-1*/*smp-1 smp-2* mutants at the L1 stage, when the proportion of cells expressing SMPs/PLX-1 in the whole body is large. In the mutants, an ~1.6-fold increase in P-eIF2α was observed (Fig. 2A), indicating that the SMPs signal is necessary to keep P-eIF2α low. Next, we prepared a *plx-1* mutant line expressing *plx-1* transcripts under a heat-shock promoter (*hs*p), and compared P-eIF2α before and after heat shock (HS). Induced expression of PLX-1 reduced P-eIF2α to a wild-type level by 2 h after HS (Fig. 2B). In addition, we analyzed P-eIF2α in a line expressing both *smp-1* and *plx-1* transcripts under *hs*p. Induced co-expression of SMP-1 and PLX-1 in the whole body of wild-type animals resulted in a reduction of P-eIF2α to 58% of a control (Fig. 2B). Thus, the reduction in P-eIF2α is indicated to be a direct and acute consequence of SMPs signaling.

Furthermore, the introduction of *gcn-1* and/or *pek-1* mutations to *plx-1* mutants reduced P-eIF2α (Fig. 2A), which correlated with the degree of suppression of the

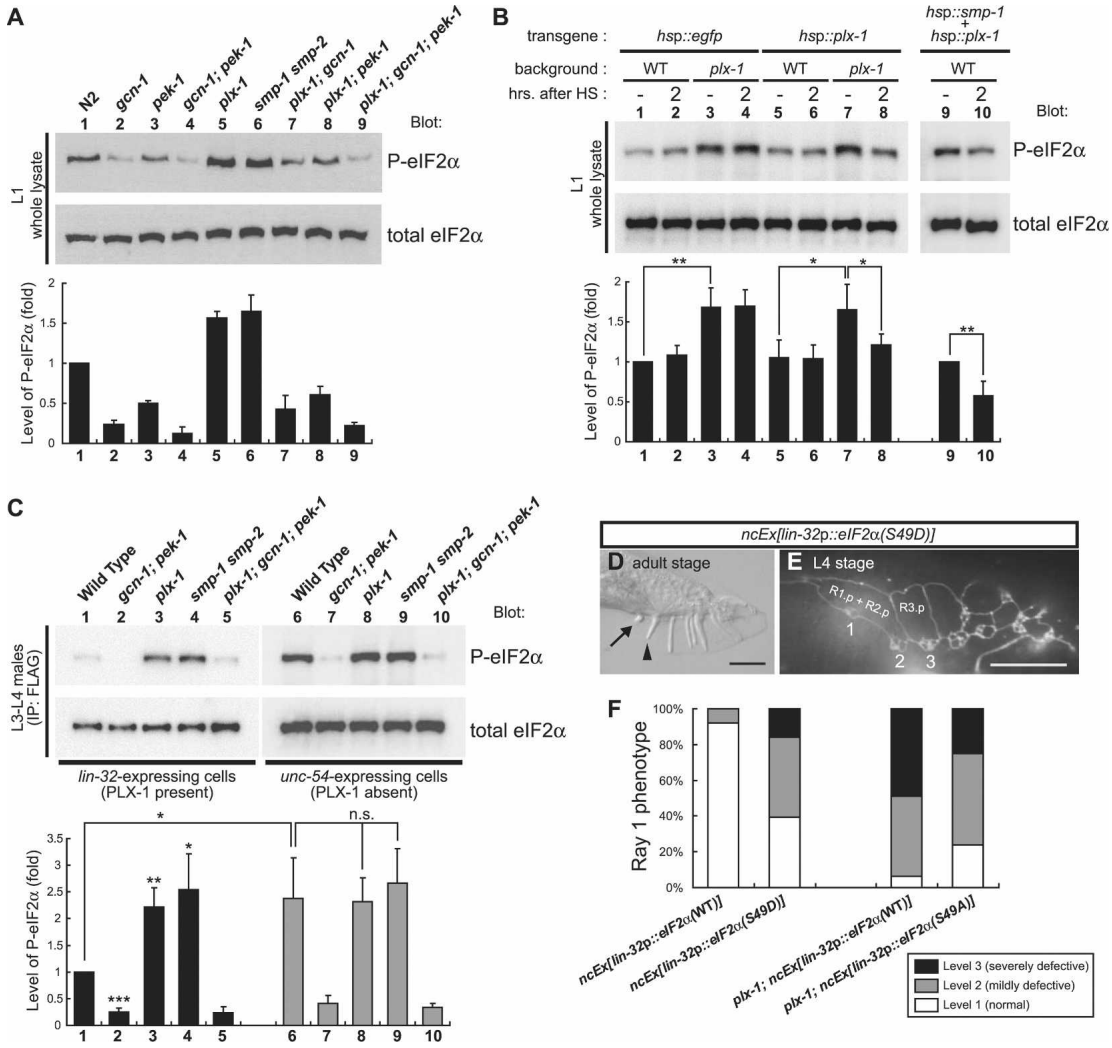

Figure 2. The SMPs signal lowers P-eIF2α, which is required for the proper ray morphogenesis. (*A*) Western blot showing the level of P-eIF2α in L1 whole animals of the indicated genotypes. The intensity of P-eIF2α normalized by total eIF2α is shown in the graph *below*. Shown are the means ± SEM of at least three independent experiments. *gcn-1* ($P < 0.001$, *t*-test) and *pek-1* ($P < 0.001$) reduce P-eIF2α, whereas *plx-1* ($P < 0.001$) and *smp-1 smp-2* ($P < 0.005$) increase it. *plx-1* slightly increases P-eIF2α in *gcn-1* ($P < 0.15$), *pek-1* ($P < 0.16$), or *gcn-1; pek-1* ($P < 0.15$). (*B*) Transient SMPs signaling acutely reduces P-eIF2α. Wild-type or *plx-1* animals at the L1 stage carrying either *hsp::egfp* (lanes *1–4*), *hsp::plx-1* (lanes *5–8*), or *hsp::smp-1* and *hsp::plx-1* (lanes *9,10*) were examined for the level of P-eIF2α. Heat-shocked samples (2) were collected 2 h after HS. Shown in the graph are the means of normalized P-eIF2α ± SEM of four independent experiments. (*C*) P-eIF2α is highly elevated in ray precursor cells. L3–L4 males carrying either *lin-32p::eIF2α::Flag* (lanes *1–5*) or *unc-54p::eIF2α::Flag* (lanes *6–10*) were collected, and Flag-tagged eIF2α proteins were immunoprecipitated and subjected to Western blot analysis. Shown in the graph are the means of normalized P-eIF2α ± SEM of three independent experiments (black bars represent P-eIF2α in *lin-32*-expressing cells; gray bars represent P-eIF2α in *unc-54*-expressing cells). (*D,E*) Forced expression of the phosphomimetic form of eIF2α, S49D, in ray precursor cells causes the ray defect similarly to *plx-1*/*smp-1 smp-2*. (*F*) Quantitative ray 1 phenotype in adult males carrying the indicated transgenes. Note that expression of the nonphosphorylatable form of eIF2α, S49A, partially suppresses the ray 1 phenotype in *plx-1*. (*) $P < 0.05$; (**) $P < 0.005$; (***) $P < 0.001$.

ray 1 phenotype. The presence of the *plx-1* mutation slightly increased P-eIF2α in *gcn-1*, *pek-1*, or *gcn-1; pek-1* mutants (Fig. 2A), indicating that neither the *gcn-1* nor *pek-1* mutation alone is completely epistatic to the *plx-1* mutation in respect to P-eIF2α. This suggests that the SMPs signal may simultaneously inactivate multiple pathways involved in the eIF2α phosphorylation, including GCN-1-dependent and PEK-1-dependent pathways. Alternatively, the signal might activate eIF2α phosphatase(s).

A semaphorin-induced reduction in the eIF2α phosphorylation is essential for the proper epidermal ray morphogenesis

To investigate further the causal relationship between P-eIF2α and the ray phenotype, we used a line expressing Flag-tagged eIF2α under the *lin-32*p and analyzed P-eIF2α in the Flag immunoprecipitates from transgenic males at the L3–L4 stage. During this period, which is crucial for ray positioning by SMPs, the majority of immunopre-

cipitated eIF2α is presumably derived from ray precursor cells (Supplemental Fig. S2). In *plx-1/smp-1 smp-2* mutants, P-eIF2α in the immunoprecipitates was elevated by ~2.5-fold (Fig. 2C), thus correlating elevated P-eIF2α and the ray defect in the mutants. P-eIF2α in the supernatant was comparable in wild-type and *plx-1/smp-1 smp-2* mutants (Supplemental Fig. S5), consistent with the limited proportion of SMPs/PLX-1-expressing cells in the whole body during this period. We also prepared another line expressing eIF2α::Flag under the promoter of *unc-54*, a gene specific to muscles, where PLX-1 expression is absent. P-eIF2α in the Flag immunoprecipitates, representing P-eIF2α in PLX-1-absent cells, was comparably high in both wild type and *plx-1/smp-1 smp-2* mutants at the L3–L4 stage (Fig. 2C). Thus, the reduction in P-eIF2α in wild-type ray precursor cells is likely to depend on SMPs signaling.

Next, we examined the phenotype in transgenic males expressing the phosphomimetic eIF2α [eIF2α(S49D)] under the *lin-32*p. Similarly to *plx-1/smp-1 smp-2* mutant males, they often exhibited a ray defect (Fig. 2D–F), suggesting that the distorted ray morphogenesis in the mutants can be attributed, at least partly, to elevated P-eIF2α. Conversely, another transgene expressing the nonphosphorylatable eIF2α [eIF2α(S49A)] partially suppressed the ray 1 phenotype in *plx-1* adults (Fig. 2F). Likewise, *gcn-1* and/or *pek-1* mutations reduced P-eIF2α in the *plx-1* mutant background in *lin-32*-expressing cells (Fig. 2C; Supplemental Fig. S6B), suggesting that suppression of the ray defect in *plx-1/smp-1 smp-2* mutants is largely dependent on reduced P-eIF2α in ray precursor cells. These results indicate that the SMPs signal serves to lower P-eIF2α in ray precursor cells, which contributes to the proper positioning of ray 1.

Having characterized the roles for GCN-1 and PEK-1, we reasoned that knockdown of a GCN2 homolog, *Y81G3A.3*, would likewise suppress the ray 1 phenotype in *plx-1/smp-1 smp-2* mutants and reduce P-eIF2α. Y81G3A.3 protein seems to have an eIF2α kinase activity as evidenced by a reduction in P-eIF2α in *Y81G3A.3* mutant whole animals (Supplemental Fig. S6B,C). Unexpectedly, however, the *Y81G3A.3* mutations neither suppressed the ray 1 phenotype in *plx-1* adults (Supplemental Fig. S6A) nor significantly reduced P-eIF2α in *lin-32*-expressing cells at the L3–L4 stage (Supplemental Fig. S6B). Thus, it is implied that Y81G3A.3 protein plays only a minor role as an eIF2α kinase in ray precursor cells and that GCN-1 signaling relies on yet-unidentified eIF2α kinase(s).

Down-regulated protein synthesis is causally related to the ray defect

Elevated P-eIF2α is known to mediate global translation inhibition as well as translation stimulation of certain mRNA species (Holcik and Sonenberg 2005), prompting us to examine whether repressed or enhanced translation causes the ray defect. eIF2 and eIF4F complexes and translation elongation factors (eEFs) play indispensable roles in translation, whereas eIF4E-binding protein (4E-BP) represses translation by interfering with eIF4E (Hershey and Merrick 2000). RNAi against eIF2α, eIF2β/*iftb-1*, eIF4G/*ifg-1* (a component of eIF4F), eEF2/*eft-1*, and eEF2/*eft-2* (Rhoads et al. 2006) all caused the growth defect, but animals that survived into the L4 and adult stages exhibited the ray defect similarly to *plx-1/smp-1 smp-2* mutants (Fig. 3). In contrast, RNAi against *spn-2*, a gene-encoding protein that has partial homology with mammalian 4E-BP and might be its counterpart in *C. elegans* (W. Li and L. Rose, pers. comm.), partially suppressed the ray 1 phenotype in *plx-1* mutants (Fig. 3G). Thus, these results argue that down-regulated translation is causally related to the ray defect in *plx-1/smp-1 smp-2* mutants.

Semaphorin preferentially stimulates translation of unc-60A/*cofilin in a manner dependent on its 3′ untranslated region (UTR)*

Having established a role for the SMPs signal in translation stimulation, what are the key translational targets?

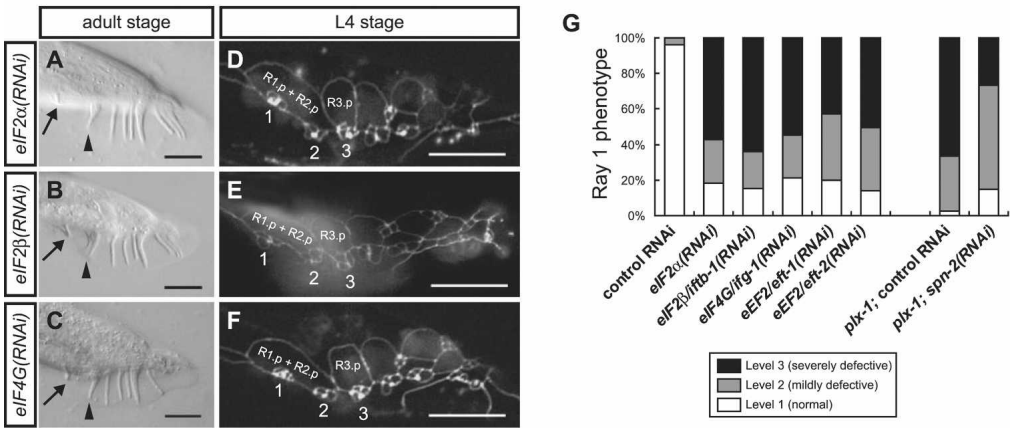

Figure 3. Down-regulated translation is causally related to the ray defect. Knockdown of translational machineries including eIF2α (*A*,*D*), eIF2β (*B*,*E*), and eIF4G (*C*,*F*) causes a ray defect. (*G*) Quantitative ray 1 phenotype in adult males treated with the indicated RNAi. Note that knockdown of eEF2 (*eft-1* and *eft-2*) causes a ray defect, while knockdown of *spn-2* partially suppresses the ray 1 phenotype in *plx-1*.

One particular candidate is ADF/cofilin, whose vertebrate ortholog is suggested to be a downstream component of Sema3A signaling (Aizawa et al. 2001; Piper et al. 2006). A *C. elegans* cofilin ortholog is encoded by *unc-60*, which produces two functionally distinct isoforms, UNC-60A and UNC-60B (Ono and Benian 1998). Since UNC-60B is expressed specifically in muscles, we turned to the analysis of ubiquitously expressed UNC-60A.

We compared the expression level of UNC-60A in L1 whole animals. In *plx-1*/*smp-1 smp-2* mutants, UNC-60A expression was decreased to 67% of wild type. The *gcn-1* mutation, which did not affect UNC-60A expression alone, restored it to 82% of wild type in the *plx-1* mutant background (Fig. 4A), consistent with the notion that reduced P-eIF2α leads to enhanced protein synthesis. The amount of *unc-60A* transcripts in L1 animals was comparable among wild type and *plx-1*/*smp-1 smp-2* mutants by Northern blot analysis (Supplemental Fig. S7), indicating that UNC-60A expression in the mutants is repressed at the translational or the post-translational level. We also analyzed the time course of SMPs-induced UNC-60A synthesis in *plx-1* mutants carrying the *hsp*::*plx-1* transgene at the L1 stage (Fig. 4B). The UNC-60A expression level did not differ from that of untreated animals at 2 h after HS, the time sufficient to rescue the elevated P-eIF2α phenotype in the mutants. At 3 and 4 h after HS, however, it increased significantly and reached a wild-type level. Thus, it is suggested that the SMPs signal acutely reduces P-eIF2α, which may in turn stimulate de novo translation of mRNAs including *unc-60A*.

Translational efficiency in a large number of mRNAs can be controlled by a regulatory sequence in their 3′UTRs (Kuersten and Goodwin 2003). To examine whether translation of *unc-60A* by SMPs signaling is dependent on its 3′UTR, which is highly conserved among nematodes (Supplemental Fig. S8), we used a line harboring chromosomally integrated reporters expressing *lin-32*p-driven *EGFP* with *unc-54* 3′UTR (*lin-32*p::*EGFP*::*unc-54* 3′UTR) and *lin-32*p-driven *mRFP* with *unc-60A* 3′UTR (*lin-32*p::*mRFP*::*unc-60A* 3′UTR) (Fig. 5A). We quantified the intensities of both fluorescence in a ray precursor unit composed of Rn.aa, Rn.ap, and Rn.p cells [collectively designated as R(n).$_{a+p}$] at the L3 stage, when their morphologies still appear unaffected in *plx-1*/*smp-1 smp-2* mutants. In wild type, both EGFP and mRFP were intensely detected in every R(n).$_{a+p}$. However, in *plx-1*/*smp-1 smp-2* mutants, EGFP intensity was decreased in most R(n).$_{a+p}$ (Fig. 5B,C). Since *unc-54* expression is absent in ray precursor cells, and thus its 3′UTR is unlikely to confer translational specificity by the SMPs signal, decreased EGFP expression in the mutants indicates globally down-regulated gene expression, consistent with elevated P-eIF2α in the mutants. Intriguingly, R(1).$_{a+p}$ and R(2).$_{a+p}$ units displayed more pronounced decreases in expression of mRFP than those of EGFP in the mutants (Fig. 5B,C), suggesting that 3′UTR of *unc-60A* mediates its preferential translation by the SMPs signal. In contrast, in R(5).$_{a+p}$, decreases in expression of mRFP were comparable with those of EGFP in the mutants (Fig. 5B,C). Similar phenotypes were observed in another line expressing *mRFP* with *unc-54* 3′UTR and *EGFP* with *unc-60A* 3′UTR under the *lin-32*p (Supplemental Fig. S9). Thus, these results suggest that the SMPs signal stimulates global translation and simultaneously activates *unc-60A* translation in a target gene- and cell type-specific manner.

Translation of unc-60A/*cofilin mediates the semaphorin-regulated ray morphogenesis*

Predominant repression of *unc-60A* 3′UTR-dependent protein expression in R(1).$_{a+p}$ and R(2).$_{a+p}$ units appears

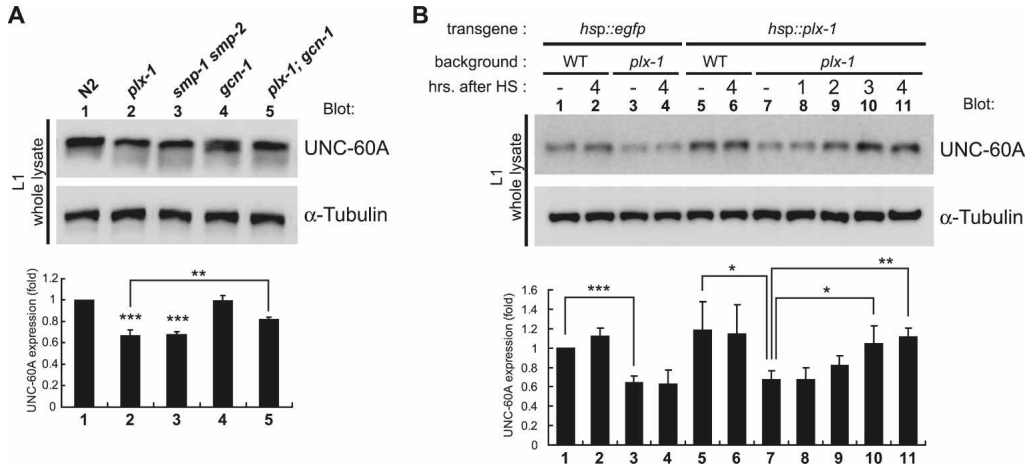

Figure 4. UNC-60A synthesis is stimulated by the SMPs signal. (*A*) Western blot showing the level of UNC-60A expression. Samples from L1 whole animals were analyzed with either anti-UNC-60A or anti-α-tubulin antibodies. UNC-60A expression normalized by α-tubulin is shown in the graph *below*. Shown are the means ± SEM of four independent experiments. (*B*) Induced expression of PLX-1 results in restoration of UNC-60A expression in *plx-1*. A similar protocol was used as in Figure 2B. Samples were collected at the indicated times after HS. Shown in the graph are the means of normalized UNC-60A expression level ± SEM of three independent experiments. (*) $P < 0.05$; (**) $P < 0.005$; (***) $P < 0.001$.

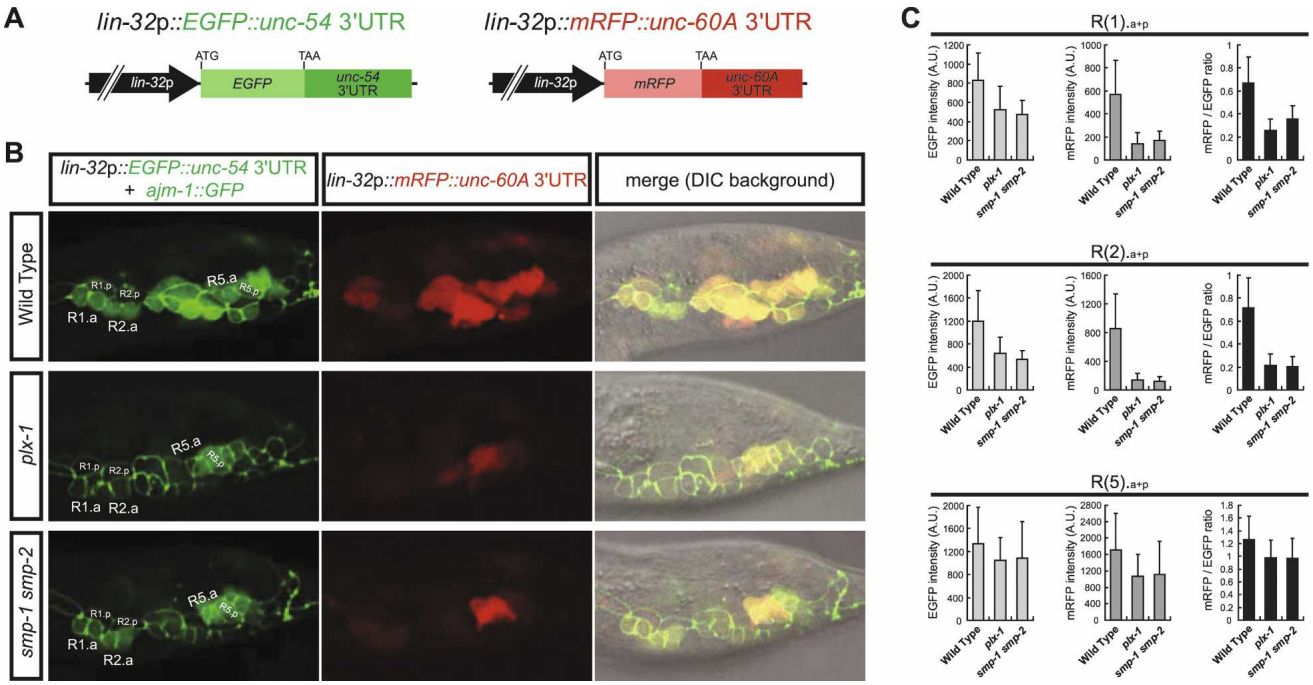

Figure 5. The SMPs signal simultaneously stimulates global translation and preferential translation of *unc-60A* via its 3′UTR in ray precursor cells. (*A*) Structures of *lin-32*p::*EGFP*::*unc-54* 3′UTR and *lin-32*p::*mRFP*::*unc-60A* 3′UTR reporter constructs. (*B*) Expression profiles of the reporter transgenes. In the *left* column, *lin-32*p-driven EGFP expression, together with AJM-1::GFP expression delineating the epidermal cell boundaries, are shown. In the *middle* column, *lin-32*p-driven mRFP expression is shown. Merged images in the DIC background are shown in the *right* column. (*C*) The fluorescent intensities of EGFP (light-gray bars) and mRFP (dark-gray bars) in arbitrary units (A.U.) and the ratio of mRFP/EGFP intensities (black bars) within $R(1)._{a+p}$, $R(2)._{a+p}$, and $R(5)._{a+p}$. Shown are the means ± SEM of 20 independent samples.

to correspond with the structural ray phenotype in *plx-1/smp-1 smp-2* mutants, leading us to suspect that *unc-60A* translation is essential for the SMPs-regulated ray morphogenesis. Consistently, RNAi against *unc-60A* caused, in addition to the growth defect, a highly penetrant ray defect similarly to the *plx-1/smp-1 smp-2* mutations (Fig. 6A–C). *unc-60A* RNAi in the *gcn-1* mutant background caused a ray defect as severely as in the wild-type background (Fig. 6C), suggesting that *unc-60A* genetically functions downstream from the translational regulation. Despite the similar ray defect as in *plx-1/smp-1 smp-2* mutants, *unc-60A* RNAi did not change P-eIF2α (Fig. 6D), implying that elevated P-eIF2α is a cause, but not a consequence, of the morphological defect in *plx-1/smp-1 smp-2* mutants.

Furthermore, expression of *unc-60A* transcripts with *unc-54* 3′UTR under the *lin-32*p (*lin-32*p::*unc-60A*::*unc-54* 3′UTR) partially suppressed the ray 1 phenotype in *plx-1/smp-1 smp-2* adults (Fig. 6E), indicating a functional link between SMPs–PLX-1 and UNC-60A during the ray morphogenesis. In contrast, *unc-60A* transcripts with *unc-60A* 3′UTR (*lin-32*p::*unc-60A*::*unc-60A* 3′UTR) failed to suppress the ray 1 phenotype in the mutants (Fig. 6E), implicating unsuccessful synthesis of UNC-60A in the absence of the SMPs signal with this transgene, which is insufficient for the proper ray morphogenesis. Taken together, we speculate that, in addition to enhancing global translation mainly by reducing P-eIF2α, the SMPs signal uses 3′UTR of *unc-60A* to allow its selective translation, and that synthesized UNC-60A regulates the epidermal morphogenesis for the proper ray 1 positioning, probably by accelerating actin cytoskeletal turnover and shaping ray precursor cells.

Discussion

Here, our study on *C. elegans* provided the in vivo demonstration that translation stimulation is an essential downstream event of the SMPs–PLX-1 signal during the cellular morphogenesis. Our genetic approach enabled us to provide several lines of evidence that the SMPs signal uses eIF2α as a major translational regulator. First, in *plx-1/smp-1 smp-2* mutants, P-eIF2α was elevated in ray precursor cells (Fig. 2C), implying down-regulated protein synthesis. Second, expression of the phosphomimetic eIF2α mimicked the ray defect in the mutants (Fig. 2D–F), suggesting that the mutant phenotype is at least partly attributed to elevated P-eIF2α. Third, the ray defect in the mutants was markedly suppressed by genetically reducing P-eIF2α (Figs. 1, 2), suggesting that up-regulated protein synthesis largely bypasses the requirement for the SMPs signal. Thus, our results reveal both requirement and sufficiency of mRNA translation stimulation via eIF2α in the SMPs-regulated epidermal ray morphogenesis.

eIF2α phosphorylation has been hitherto regarded as a

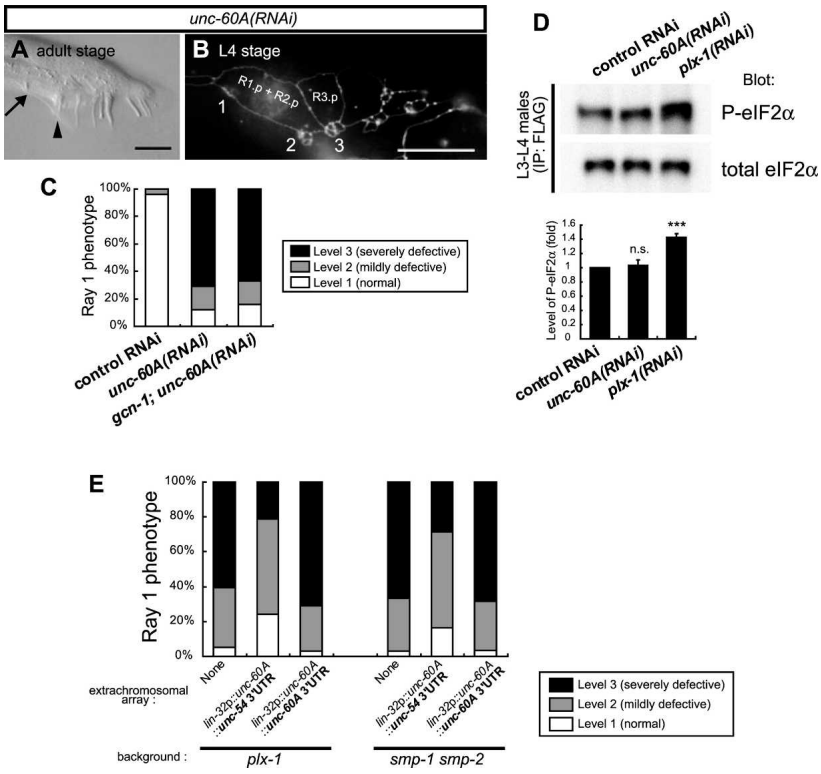

Figure 6. UNC-60A mediates the SMPs-regulated ray morphogenesis. (*A*,*B*) Knockdown of *unc-60A* phenocopies *plx-1/smp-1 smp-2*. (*C*) Quantitative ray 1 phenotype in adult males of the indicated genotypes. (*D*) Knockdown of *unc-60A* does not elevate the level of P-eIF2α. Samples treated with the indicated RNAi were collected as in Figure 2C, and the Flag immunoprecipitates were subjected to Western blot analysis. Shown in the graph are the means of normalized P-eIF2α ± SEM of three independent experiments. (***) $P < 0.001$. (*E*) Quantitative ray 1 phenotype in *plx-1/smp-1 smp-2* mutant adults carrying the indicated transgenes. Note that expression of *unc-60A* transcripts fused with *unc-54* 3′UTR, but not with *unc-60A* 3′UTR, partially suppresses the ray 1 phenotype in the mutants.

stress-induced event, and its involvement in semaphorin signaling is unexpected. Our results, however, indicate a direct effect of the SMPs signal on reducing P-eIF2α. Forced expression of SMP-1 and PLX-1 was sufficient to quickly reduce P-eIF2α in otherwise normal wild-type animals (Fig. 2B), indicating that increase in P-eIF2α in *plx-1/smp-1 smp-2* mutants is not a consequence of possible cellular stresses due to morphological defects in the mutants, but is caused by failure to reduce P-eIF2α due to lack of SMPs signaling. This notion is supported by the finding that P-eIF2α in PLX-1-expressing ray precursor cells is lower than that in PLX-1-absent muscle cells (Fig. 2C). In agreement with our proposal, independent studies have revealed that BDNF treatment (Takei et al. 2001), fibroblast adhesion (Gorrini et al. 2005), and L-LTP-inducing protocol (Costa-Mattioli et al. 2005, 2007) enhance translation by reducing P-eIF2α. The regulation of P-eIF2α also has physiological roles in various developmental events (Harding et al. 2001; Shen et al. 2001; Fang et al. 2003), which indicates the involvement of signals unrelated to stress in multiple aspects of eIF2α-mediated biological processes.

Suppression of the ray defect in *plx-1/smp-1 smp-2* mutants by *gcn-1; pek-1* mutation was highly but not fully penetrant (Fig. 1I), despite the fact that P-eIF2α in the mutants was even lower than that in wild type (Fig. 2C), implicating mechanism(s) other than the eIF2α regulation as another branch of SMPs signaling. The finding of selective translation via *unc-60A* mRNA 3′UTR by the SMPs signal (Fig. 5; Supplemental Fig. S9) also suggests this possibility (discussed below). Considering our findings that knockdown of eIF4G phenocopied *plx-1/smp-1 smp-2* mutants and that knockdown of putative 4E-BP, *spn-2*, partially suppressed the ray 1 phenotype in *plx-1* mutants (Fig. 3), eIF4F complex formation might be another possible target event of SMPs signaling. This speculation agrees with the previous finding that eIF4F complex formation is regulated by Sema3A via mTOR, a well-known eIF4F regulator, in vertebrate neurons (Campbell and Holt 2001). Thus, we hypothesize that the SMPs signal up-regulates translation by reducing P-eIF2α and simultaneously activating eIF4F complex during the ray morphogenesis. Indeed, other studies have shown that eIF2 complex and eIF4F complex formations are sometimes regulated coordinately (Takei et al. 2001; Gorrini et al. 2005), and that there is a cross-talk between eIF2α and TOR (Cherkasova and Hinnebusch 2003; Kubota et al. 2003). Given that both complex formations are the rate-limiting steps in translation (Hershey and Merrick 2000), this hypothesis appears reasonable.

We identified cofilin/UNC-60A as a potent target synthesized in response to the SMPs signal (Fig. 4), which coincides with the recent report on rapid cofilin synthesis by Sema3A application in vertebrate neurons (Piper et al. 2006). Aizawa et al. (2001) reported that Sema3A induces a rapid elevation and a subsequent reduction in the cofilin phosphorylation during the growth cone collapse, indicating the importance of a cycle of cofilin between activation and inactivation. It is not known whether such an activation–inactivation cycle exists for UNC-60A in *C. elegans*, whose genome lacks any genes for a cofilin kinase LIM-kinase (Arber et al. 1998; Yang et al. 1998) and a phosphatase, Slingshot (Niwa et al. 2002).

Nevertheless, UNC-60A is known to play a role in F-actin depolymerization (Ono and Benian 1998), which we consider may be important for the arrangement of ray precursor cells as a downstream event of SMPs signaling. It is documented that each ray precursor cluster is positioned at the junctional site between two adjacent Rn.ps (Baird et al. 1991). Indeed, in *plx-1* mutants, the boundary between R1.p and R2.p shifts anteriorly, causing the anterior displacement of ray precursor cluster 1 to its normal position (Fujii et al. 2002). Notably, we found that in R(1)$._{a+p}$ and R(2)$._{a+p}$ units of *plx-1/smp-1 smp-2* mutants, prominent repression of *unc-60A* 3′UTR-dependent translation appeared to precede their defective morphogenesis (Fig. 5; Supplemental Fig. S9), suggesting that down-regulated UNC-60A expression is a major cause of the structural ray phenotype. Expectedly, *unc-60A* knockdown phenocopied *plx-1/smp-1 smp-2* mutants, and forced expression of UNC-60A partially suppressed the ray defect in the mutants (Fig. 6). In contrast to R(1)$._{a+p}$ and R(2)$._{a+p}$, the SMPs signal appeared to have a relatively minor effect on *unc-60A* 3′UTR-dependent translation in the R(5)$._{a+p}$ unit (Fig. 5), which could account for the apparent lack of positional defects in ray 5 in *plx-1/smp-1 smp-2* mutants. Taken together, we propose that the SMPs signal preferentially stimulates UNC-60A synthesis in R1.p and R2.p, and hence determines the position of ray 1 by posteriorly shifting the boundary between the two cells.

In cultured vertebrate growth cones, guidance cues rapidly activate translation in minutes at the site close to their application (Campbell and Holt 2001). Although our Western blot analysis using the *hs*p::*plx-1* rescue construct showed that *unc-60A* translation is initiated by 2–4 h after HS (Figs. 2B, 4B), the time necessary for the production of functional PLX-1 molecules after HS is not known, leaving the likely time scale of the SMPs translation events in the epidermal system undetermined. Considering that R1.p makes contact with R2.p until their fusion, and that PLX-1 expression in ray precursor cells lasts throughout their development (Fujii et al. 2002), the SMPs signal may stimulate protein synthesis, including UNC-60A, continuously, rather than transiently. Future examination of the spatiotemporal pattern of signaling events would provide further clues to the mechanism of cellular morphogenesis regulated by SMPs-induced UNC-60A synthesis.

In cultured vertebrate neurons, several guidance cues activate the common translational regulators (eIF4E and 4E-BP1), but they stimulate synthesis of different kinds of proteins that generate distinct cellular responses, depending on whether they are attractive cues or repulsive ones (Wu et al. 2005; Leung et al. 2006; Piper et al. 2006). mRNAs for cytoskeletal regulators/components like β-actin (Zhang et al. 2001; Leung et al. 2006) and RhoA (Wu et al. 2005), for instance, contain motifs in their 3′UTRs that are implicated in their selective translation in response to these cues. Similarly to such gene-specific regulation, we found preferential stimulation of *unc-60A* 3′UTR-dependent translation by the SMPs signal. Since in most of the known cases 3′UTR-mediated translational regulation involves the interference with eIF4F assembly at the 5′ cap of mRNAs by 3′UTR-binding translational repressors, the SMPs signal might inhibit the repressors so as to enable the preferential *unc-60A* mRNA translation. This idea is supported by the presence of a putative cytoplasmic polyadenylation element (CPE) in its 3′UTR (Supplemental Fig. S8), a consensus sequence that, via its binding protein CPEB, can be targeted by such translational repressors (Mendez and Richter 2001). An alternative unprecedented idea is that the SMPs signal might stimulate 3′UTR-dependent *unc-60A* translation via the regulation of eIF2α. A possible scenario would be that eIF2 ternary complex binding to the 40S ribosomal subunit in the 43S preinitiation complex is destabilized in the presence of the presumptive factors bound to *unc-60A* 3′UTR, which can be overcome as the SMPs signal lowers eIF2α phosphorylation and increases the level of ternary complex formation.

Only partial suppression of the ray 1 phenotype in *plx-1/smp-1 smp-2* mutants by UNC-60A expression (Fig. 6E) implies that a protein other than UNC-60A is also synthesized by and required for SMPs signaling. Other cytoskeletal regulators/components might be possible targets of translational regulation. One candidate is RhoA, whose transcripts display localized distribution to the axonal tips, where they are translated by Sema3A in mammals (Wu et al. 2005). Interestingly, knockdown of *C. elegans* RhoA, *rho-1*, was reported to produce a mildly penetrant ray 1 phenotype similarly to *plx-1/smp-1 smp-2* mutants (Dalpe et al. 2004).

To summarize, we provided lines of in vivo evidence that the SMPs signal stimulates mRNA translation. The signal reduces P-eIF2α and, as our data infer, may concertedly activate eIF4F complex formation, which leads to global translation combined with selective translation as illustrated with *unc-60A* in a manner dependent on its 3′UTR. Together with accumulating evidence in the nervous system (Wu et al. 2005; Leung et al. 2006; Piper et al. 2006; Schratt et al. 2006; Lin and Holt 2007), our results imply that translation of mRNA species, especially those relevant to cytoskeleton, is a fundamental mechanism for regulating cell morphology.

Materials and methods

Strains

Standard techniques for *C. elegans* culture and genetics were used as described by Brenner (1974). For analysis of the male tails, strains carried the *him-5* mutation. For Western blot and Northern blot analyses, N2 was used as a wild-type control, unless otherwise noted. The following alleles were used: [LGI] *smp-1(ev715)*, *smp-2(ev709)*; [LGII] *rrf-3(pk1426)*, *Y81G3A.3 (tm1267*, *ok871*, *ok886)*, *ncIs13[ajm-1*::*gfp]*; [LGIII] *gcn-1(nc40)*, *tDf9*; [LGIV] *plx-1(nc37*, *ev724)*, *jcIs1[ajm-1*::*gfp; unc-29(+); rol-6(su1006)]*; [LGV] *him-5(e1490)*; [LGX] *pek-1(ok275*, *tm629)*; Bristol N2; Hawaiian CB4856. The linkage groups of *ncIs17[hs*p::*egfp]*, *ncIs19[hs*p::*plx-1; hs*p::*egfp; rol-6(su1006)]*, *ncIs32[lin-32*p::*mRFP*::*unc-54* 3′UTR*; lin-32*p::*EGFP*::*unc-60A* 3′UTR*; rol-6(su1006)]*, and *ncIs33[lin-32*p::*EGFP*::*unc-54* 3′UTR*; lin-32*p::*mRFP*::*unc-60A* 3′UTR*; rol-6(su1006)]* have not been determined.

Isolation of suppressor mutants

Young adult *plx-1(nc37); him-5(e1490)* mutants were mutagenized with ethylmethane sulfonate (EMS). Males from F3 progeny representing up to 1000 haploid genomes were screened under Nomarski optics (Zeiss Axioplan) to examine whether the ray 1 anterior displacement characteristic of *plx-1; him-5* was suppressed. One of the isolated suppressor mutants, *plx-1; him-5; nc40*, was out-crossed 10 times to *plx-1; him-5*. *nc40* single mutants were fertile and appeared healthy, but the brood size was reduced to half (N2: 358 ± 23; *nc40*: 178 ± 28 [$n = 3$ for each]).

Genetic mapping of nc40

Two-factor and three-factor crosses mapped *nc40* at 1.4 map units right to *dpy-1* on linkage group III. Further mapping was performed by using single nucleotide polymorphisms (SNPs) between N2 and CB4856 strains. F2 progeny from *plx-1; him-5; nc40* (N2 background) × *plx-1; him-5* (CB4856 background) crosses were isolated, and populations were generated from each isolate. Male tails from each population were tested to determine the genotype of the suppressor gene. Genomic DNA was prepared from each population, which was either wild type or homozygous *nc40*, and SNPs were scored by PCR amplification followed by restriction enzyme digestion or sequencing. Using genomic DNA from 72 populations, *nc40* was mapped between nucleotides 84,618 and 108,185 on Y48G9A.

RNAi

Genomic DNA fragments of *gcn-1* (Y48G9A: nucleotides 105,712–106,114), *eIF2*α (Y37E3: 14,315–14,862), *eIF2*β*/iftb-1* (C54G4: 34,320–K04G2: 287), *eIF4G/ifg-1* (M110: 15,908–16,949), *eEF2/eft-1* (ZK328: 13,513–15,136), *eEF2/eft-2* (F25H5: 10,535–11,429), *spn-2* (F56F3: 21,390–22,631), *unc-60A* (C38C3: 19–1074), 3′UTR of *unc-60A* (C38C3: 976–1682), and a cDNA fragment of *plx-1* (nucleotides 603–1912) were subcloned into the pPD129.36 vector, and the resulting constructs were transformed into HT115 bacteria to allow for the synthesis of dsRNA in the presence of 1 mM IPTG (Timmons and Fire 1998). Young adult hermaphrodites were fed with the transformed bacteria, and the F1 progeny were analyzed for their phenotypes. Animals carried the *rrf-3(pk1426)* mutation, which gives hypersensitivity to RNAi (Simmer et al. 2002) but does not affect the morphology of male tails alone. Animals fed with bacteria harboring the empty pPD129.36 vector were used as controls.

*Generation of anti-eIF2*α *antibody*

A rabbit polyclonal antibody was raised against a synthetic peptide corresponding to 16 amino acid residues near the C terminus of *C. elegans* eIF2α (BioGate). The peptide consisted of NH_2-VDAEEASRDNRKKAGD-COOH and was coupled to keyhole limpet hemocyanin. The antibody specifically labels *C. elegans* eIF2α protein, as evidenced by the disappearance of a 39-kDa immunoblot signal in *eIF2*α*(RNAi)* animals (data not shown).

Immunoprecipitation

L3 and L4 males were collected in lysis buffer containing 50 mM Tris (pH 7.4), 150 mM NaCl, 1 mM EDTA, 1% Triton X-100, 1 mM PMSF, and protease inhibitor cocktail (Sigma), and dissolved by brief sonication and incubation with a rotator for 1 h at room temperature. Flag-tagged proteins were immunoprecipitated with anti-Flag M2 affinity gel (Sigma) according to Sigma's instructions. Both immunoprecipitates and supernatants were subjected to Western blot analysis.

Western blot analysis

Samples (8 or 20 µg of total proteins per lane) were separated by SDS–polyacrylamide gel electrophoresis and transferred to an Immobilon-P PVDF membrane (Millipore). Western blots were probed with anti-eIF2α, anti-phopho-eIF2α (Cell Signaling Technology), anti-α-tubulin (Woods et al. 1989), or anti-UNC-60A (Ono and Benian 1998) primary antibodies. The immunoblot signals were then visualized by incubation with anti-mouse or anti-rabbit IgG antibodies conjugated with horseradish peroxidase (HRP) (Cell Signaling Technology) followed by detection with an Immobilon Western chemiluminescent HRP substrate (Millipore). Images were captured and quantified with Luminescent Image Analyzer LAS-1000 (FujiFilm). One-way ANOVA was used to evaluate differences in the signal intensities.

Confocal laser microscopy

Confocal images were captured and quantified with an Olympus Fluoview300 to analyze the expression profiles of EGFP and mRFP in the male tails of *ncIs32* or *ncIs33* at the L3 stage, when each ray precursor unit, $R(n)._{a+p}$, is composed of one Rn.p cell and two Rn.a descendants, Rn.aa and Rn.ap cells. Cell boundaries were delineated with *ncIs13[ajm-1::gfp]*. In each observation, the same laser intensity and exposure conditions were used. As a reference, the fluorescent intensity of an AVM cell body was measured. AVM, which does not express *plx-1*, gave an indistinguishable value in each observation (data not shown).

Acknowledgments

We thank the staff of Fujisawa and Oda Laboratories, Hiromi Hirata, Kunihiro Matsumoto, Naoki Hisamoto, and Jonathan Ewbank for discussion and comments; Mie Chikuma for *nc40* mapping; Motoshi Suzuki for constructing *ncIs17* and *ncIs19*; Yuji Kohara for cDNA clones; Andrew Fire for pPD49.26 and other vectors; Shoichiro Ono for anti-UNC-60A antibody; Keith Gull for anti-α-tubulin antibody; Roger Tsien and Hiroshi Kagoshima for mRFP cDNA; Lesilee S. Rose for information on *spn-2*; and Douglas S. Portman for information on *lin-32*p. Some strains were provided by the *Caenorhabditis* Genetic Center, which is funded by the National Institutes for Health National Center for Research Resources, and National Bioresource Project funded by the Ministry of Education, Culture, Sports, Science and Technology of Japan. This work was supported by grants from the Ministry of Education, Culture, Sports, Science and Technology of Japan (to H.F., T.I., Y.O., and S.T.); a grant from CREST (Core Research for Evolutional Science and Technology) of the Japan Science and Technology Corporation (JST) (to H.F.); and a grant from The Sumitomo Foundation (to S.T.).

References

Aizawa, H., Wakatsuki, S., Ishii, A., Moriyama, K., Sasaki, Y., Ohashi, K., Sekine-Aizawa, Y., Sehara-Fujisawa, A., Mizuno, K., Goshima, Y., et al. 2001. Phosphorylation of cofilin by LIM-kinase is necessary for semaphorin 3A-induced growth cone collapse. *Nat. Neurosci.* **4:** 367–373.

Arber, S., Barbayannis, F.A., Hanser, H., Schneider, C., Stanyon, C.A., Bernard, O., and Caroni, P. 1998. Regulation of actin dynamics through phosphorylation of cofilin by LIM-kinase.

Nature **393:** 805–809.

Baird, S.E., Fitch, D.H., Kassem, I.A., and Emmons, S.W. 1991. Pattern formation in the nematode epidermis: Determination of the arrangement of peripheral sense organs in the *C. elegans* male tail. *Development* **113:** 515–526.

Brenner, S. 1974. The genetics of *Caenorhabditis elegans*. *Genetics* **77:** 71–94.

Campbell, D.S. and Holt, C.E. 2001. Chemotropic responses of retinal growth cones mediated by rapid local protein synthesis and degradation. *Neuron* **32:** 1013–1026.

Cherkasova, V.A. and Hinnebusch, A.G. 2003. Translational control by TOR and TAP42 through dephosphorylation of eIF2α kinase GCN2. *Genes & Dev.* **17:** 859–872.

Costa-Mattioli, M., Gobert, D., Harding, H., Herdy, B., Azzi, M., Bruno, M., Bidinosti, M., Ben Mamou, C., Marcinkiewicz, E., Yoshida, M., et al. 2005. Translational control of hippocampal synaptic plasticity and memory by the eIF2α kinase GCN2. *Nature* **436:** 1166–1173.

Costa-Mattioli, M., Gobert, D., Stern, E., Gamache, K., Colina, R., Cuello, C., Sossin, W., Kaufman, R., Pelletier, J., Rosenblum, K., et al. 2007. eIF2α phosphorylation bidirectionally regulates the switch from short- to long-term synaptic plasticity and memory. *Cell* **129:** 195–206.

Dalpe, G., Zhang, L.W., Zheng, H., and Culotti, J.G. 2004. Conversion of cell movement responses to Semaphorin-1 and Plexin-1 from attraction to repulsion by lowered levels of specific RAC GTPases in *C. elegans*. *Development* **131:** 2073–2088.

Emmons, S.W. 2005. Male development. In *WormBook* (ed. The *C. elegans* Research Community), *WormBook*, doi: 10.1895/wormbook.1.33.1, http://www.wormbook.org.

Fan, J. and Raper, J.A. 1995. Localized collapsing cues can steer growth cones without inducing their full collapse. *Neuron* **14:** 263–274.

Fang, R., Xiong, Y., and Singleton, C.K. 2003. IfkA, a presumptive eIF2 α kinase of Dictyostelium, is required for proper timing of aggregation and regulation of mound size. *BMC Dev. Biol.* **3:** 3. doi: 10.1186/1471-213X-3-3.

Fujii, T., Nakao, F., Shibata, Y., Shioi, G., Kodama, E., Fujisawa, H., and Takagi, S. 2002. *Caenorhabditis elegans* PlexinA, PLX-1, interacts with transmembrane semaphorins and regulates epidermal morphogenesis. *Development* **129:** 2053–2063.

Gingras, A.C., Raught, B., and Sonenberg, N. 1999. eIF4 initiation factors: Effectors of mRNA recruitment to ribosomes and regulators of translation. *Annu. Rev. Biochem.* **68:** 913–963.

Ginzburg, V.E., Roy, P.J., and Culotti, J.G. 2002. Semaphorin 1a and semaphorin 1b are required for correct epidermal cell positioning and adhesion during morphogenesis in *C. elegans*. *Development* **129:** 2065–2078.

Gorrini, C., Loreni, F., Gandin, V., Sala, L.A., Sonenberg, N., Marchisio, P.C., and Biffo, S. 2005. Fibronectin controls cap-dependent translation through β1 integrin and eukaryotic initiation factors 4 and 2 coordinated pathways. *Proc. Natl. Acad. Sci.* **102:** 9200–9205.

Goshima, Y., Nakamura, F., Strittmatter, P., and Strittmatter, S.M. 1995. Collapsin-induced growth cone collapse mediated by an intracellular protein related to UNC-33. *Nature* **376:** 509–514.

Harding, H.P., Zeng, H., Zhang, Y., Jungries, R., Chung, P., Plesken, H., Sabatini, D.D., and Ron, D. 2001. Diabetes mellitus and exocrine pancreatic dysfunction in perk$^{-/-}$ mice reveals a role for translational control in secretory cell survival. *Mol. Cell* **7:** 1153–1163.

Hershey, J.W.B. and Merrick, W.C. 2000. Pathway and mechanism of initiation of protein synthesis. In *Translational control of gene expression* (eds. N. Sonenberg et al.), pp. 33–88. Cold Spring Harbor Laboratory Press, Cold Spring Harbor, New York.

Hinnebusch, A.G. 2000. Mechanism and regulation of initiator methyonyl-tRNA binding to ribosomes. In *Translational control of gene expression* (eds. N. Sonenberg et al.), pp. 185–243. Cold Spring Harbor Laboratory Press, Cold Spring Harbor, New York.

Holcik, M. and Sonenberg, N. 2005. Translational control in stress and apoptosis. *Nat. Rev. Mol. Cell Biol.* **6:** 318–327.

Jin, Z. and Strittmatter, S.M. 1997. Rac1 mediates collapsin-1-induced growth cone collapse. *J. Neurosci.* **17:** 6256–6263.

Kruger, R.P., Aurandt, J., and Guan, K.L. 2005. Semaphorins command cells to move. *Nat. Rev. Mol. Cell Biol.* **6:** 789–800.

Kubota, H., Obata, T., Ota, K., Sasaki, T., and Ito, T. 2003. Rapamycin-induced translational derepression of GCN4 mRNA involves a novel mechanism for activation of the eIF2 α kinase GCN2. *J. Biol. Chem.* **278:** 20457–20460.

Kuersten, S. and Goodwin, E.B. 2003. The power of the 3′ UTR: Translational control and development. *Nat. Rev. Genet.* **4:** 626–637.

Kuhn, T.B., Brown, M.D., Wilcox, C.L., Raper, J.A., and Bamburg, J.R. 1999. Myelin and collapsin-1 induce motor neuron growth cone collapse through different pathways: Inhibition of collapse by opposing mutants of rac1. *J. Neurosci.* **19:** 1965–1975.

Leung, K.M., van Horck, F.P., Lin, A.C., Allison, R., Standart, N., and Holt, C.E. 2006. Asymmetrical β-actin mRNA translation in growth cones mediates attractive turning to netrin-1. *Nat. Neurosci.* **9:** 1247–1256.

Lin, A.C. and Holt, C.E. 2007. Local translation and directional steering in axons. *EMBO J.* **26:** 3729–3736.

Marton, M.J., Crouch, D., and Hinnebusch, A.G. 1993. GCN1, a translational activator of GCN4 in *Saccharomyces cerevisiae*, is required for phosphorylation of eukaryotic translation initiation factor 2 by protein kinase GCN2. *Mol. Cell. Biol.* **13:** 3541–3556.

Mendez, R. and Richter, J.D. 2001. Translational control by CPEB: A means to the end. *Nat. Rev. Mol. Cell Biol.* **2:** 521–529.

Mohler, W.A., Simske, J.S., Williams-Masson, E.M., Hardin, J.D., and White, J.G. 1998. Dynamics and ultrastructure of developmental cell fusions in the *Caenorhabditis elegans* hypodermis. *Curr. Biol.* **8:** 1087–1090.

Nakao, F., Hudson, M.L., Suzuki, M., Peckler, Z., Kurokawa, R., Liu, Z., Gengyo-Ando, K., Nukazuka, A., Fujii, T., Suto, F., et al. 2007. The PLEXIN PLX-2 and the ephrin EFN-4 have distinct roles in MAB-20/Semaphorin 2A signaling in *Caenorhabditis elegans* morphogenesis. *Genetics* **176:** 1591–1607.

Niwa, R., Nagata-Ohashi, K., Takeichi, M., Mizuno, K., and Uemura, T. 2002. Control of actin reorganization by Slingshot, a family of phosphatases that dephosphorylate ADF/cofilin. *Cell* **108:** 233–246.

Oinuma, I., Ishikawa, Y., Katoh, H., and Negishi, M. 2004. The Semaphorin 4D receptor Plexin-B1 is a GTPase activating protein for R-Ras. *Science* **305:** 862–865.

Ono, S. and Benian, G.M. 1998. Two *Caenorhabditis elegans* actin depolymerizing factor/cofilin proteins, encoded by the unc-60 gene, differentially regulate actin filament dynamics. *J. Biol. Chem.* **273:** 3778–3783.

Piper, M., Anderson, R., Dwivedy, A., Weinl, C., van Horck, F., Leung, K.M., Cogill, E., and Holt, C. 2006. Signaling mechanisms underlying Slit2-induced collapse of *Xenopus* retinal

growth cones. *Neuron* **49:** 215–228.
Portman, D.S. and Emmons, S.W. 2000. The basic helix–loop–helix transcription factors LIN-32 and HLH-2 function together in multiple steps of a *C. elegans* neuronal sublineage. *Development* **127:** 5415–5426.
Rhoads, R.E., Dinkova, T.D., and Korneeva, N.L. 2006. Mechanism and regulation of translation in *C. elegans*. In *WormBook* (ed. The *C. elegans* Research Community), *WormBook*, doi: 10.1895/wormbook.1.63.1, http://www.wormbook.org.
Rohm, B., Rahim, B., Kleiber, B., Hovatta, I., and Puschel, A.W. 2000. The semaphorin 3A receptor may directly regulate the activity of small GTPases. *FEBS Lett.* **486:** 68–72.
Ron, D. and Harding, H.P. 2000. PERK and tranlational control by stress in the endoplasmic reticulum. In *Translational control of gene expression* (eds. N. Sonenberg et al.), pp. 547–560. Cold Spring Harbor Laboratory Press, Cold Spring Harbor, New York.
Sattlegger, E. and Hinnebusch, A.G. 2000. Separate domains in GCN1 for binding protein kinase GCN2 and ribosomes are required for GCN2 activation in amino acid-starved cells. *EMBO J.* **19:** 6622–6633.
Schratt, G.M., Tuebing, F., Nigh, E.A., Kane, C.G., Sabatini, M.E., Kiebler, M., and Greenberg, M.E. 2006. A brain-specific microRNA regulates dendritic spine development. *Nature* **439:** 283–289.
Shen, X., Ellis, R.E., Lee, K., Liu, C.Y., Yang, K., Solomon, A., Yoshida, H., Morimoto, R., Kurnit, D.M., Mori, K., et al. 2001. Complementary signaling pathways regulate the unfolded protein response and are required for *C. elegans* development. *Cell* **107:** 893–903.
Simmer, F., Tijsterman, M., Parrish, S., Koushika, S.P., Nonet, M.L., Fire, A., Ahringer, J., and Plasterk, R.H. 2002. Loss of the putative RNA-directed RNA polymerase RRF-3 makes *C. elegans* hypersensitive to RNAi. *Curr. Biol.* **12:** 1317–1319.
Sulston, J.E., Albertson, D.G., and Thomson, J.N. 1980. The *Caenorhabditis elegans* male: Postembryonic development of nongonadal structures. *Dev. Biol.* **78:** 542–576.
Takei, N., Kawamura, M., Hara, K., Yonezawa, K., and Nawa, H. 2001. Brain-derived neurotrophic factor enhances neuronal translation by activating multiple initiation processes: Comparison with the effects of insulin. *J. Biol. Chem.* **276:** 42818–42825.
Timmons, L. and Fire, A. 1998. Specific interference by ingested dsRNA. *Nature* **395:** 854.
Turner, L.J., Nicholls, S., and Hall, A. 2004. The activity of the plexin-A1 receptor is regulated by Rac. *J. Biol. Chem.* **279:** 33199–33205.
Woods, A., Sherwin, T., Sasse, R., MacRae, T.H., Baines, A.J., and Gull, K. 1989. Definition of individual components within the cytoskeleton of *Trypanosoma brucei* by a library of monoclonal antibodies. *J. Cell Sci.* **93:** 491–500.
Wu, K.Y., Hengst, U., Cox, L.J., Macosko, E.Z., Jeromin, A., Urquhart, E.R., and Jaffrey, S.R. 2005. Local translation of RhoA regulates growth cone collapse. *Nature* **436:** 1020–1024.
Yang, N., Higuchi, O., Ohashi, K., Nagata, K., Wada, A., Kangawa, K., Nishida, E., and Mizuno, K. 1998. Cofilin phosphorylation by LIM-kinase 1 and its role in Rac-mediated actin reorganization. *Nature* **393:** 809–812.
Zanata, S.M., Hovatta, I., Rohm, B., and Puschel, A.W. 2002. Antagonistic effects of Rnd1 and RhoD GTPases regulate receptor activity in Semaphorin 3A-induced cytoskeletal collapse. *J. Neurosci.* **22:** 471–477.
Zhang, H.L., Eom, T., Oleynikov, Y., Shenoy, S.M., Liebelt, D.A., Dictenberg, J.B., Singer, R.H., and Bassell, G.J. 2001. Neurotrophin-induced transport of a β-actin mRNP complex increases β-actin levels and stimulates growth cone motility. *Neuron* **31:** 261–275.